Heliyon 10 (2024) e29480

Contents lists available at ScienceDirect

Heliyon

journal homepage: www.cell.com/heliyon

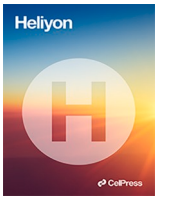

Research article

Optimal timing for drug delivery into the hippocampus by focused ultrasound: A comparison of hydrophilic and lipophilic compounds

Younghee Seo [a,b], Kyung Won Chang [a], Jihyeon Lee [c], Chanho Kong [a], Jaewoo Shin [d], Jin Woo Chang [a,b], Young Cheol Na [a,e,**], Won Seok Chang [a,*]

[a] Department of Neurosurgery and Brain Research Institute, Yonsei University College of Medicine, Seoul, South Korea
[b] Brain Korea 21 Project for Medical Science, Yonsei University College of Medicine, Seoul, South Korea
[c] Celros Biotech, Seoul, South Korea
[d] Medical Device Development Center, Daegu-Gyeongbuk Medical Innovation Foundation (K-MEDI Hub), Daegu, 41061, South Korea
[e] Department of Neurosurgery, Catholic Kwandong University College of Medicine, International St. Mary's Hospital, Incheon Metropolitan City, South Korea

ARTICLE INFO

Keywords:
Blood-brain barrier
Focused ultrasound
tight junction
Caveolae
Major facilitator superfamily domain-containing 2a (Mfsd2a)
Transcytosis

ABSTRACT

Aims: Previous studies have reported that focused ultrasound (FUS) helps modulate the blood-brain barrier (BBB). These studies have generally used the paracellular pathway owing to tight junction proteins (TJPs) regulation. However, BBB transport pathways also include diffusion and transcytosis. Few studies have examined transcellular transport across endothelial cells. We supposed that increased BBB permeability caused by FUS may affect transcytosis. We investigated drug delivery through transcytosis and paracellular transport to the brain after BBB modulation using FUS.

Main methods: FUS and microbubbles were applied to the hippocampus of rats, and were euthanized at 1, 4, 24, and 48 h after sonication. To investigate paracellular transport, we analyzed TJPs, including zona occludens-1 (ZO-1) and occludin. We also investigated caveola-mediated transcytosis by analyzing caveola formation and major facilitator superfamily domain-containing 2a (Mfsd2a) levels, which inhibit caveola vesicle formation.

Key findings: One hour after FUS, ZO-1 and occludin expression was the lowest and gradually increased over time, returning to baseline 24 h after FUS treatment. Compared with that of TJPs, caveola formation started to increase 1 h after FUS treatment and peaked at 4 h after FUS treatment before returning to baseline by 48 h after FUS treatment. Decreased Mfsd2a levels were observed at 1 h and 4 h after FUS treatment, indicating increased caveola formation.

Significance: FUS induces BBB permeability changes and regulates both paracellular transport and caveola-mediated transcytosis. However, a time difference was observed between these two mechanisms. Hence, when delivering drugs into the brain after FUS, the optimal drug administration timing should be determined by the mechanism by which each drug passes through the BBB.

* Corresponding author. Department of Neurosurgery Yonsei University College of Medicine 50 Yonsei-ro, Seodaemun-gu, Seoul, 03722, South Korea.

** Corresponding author. Catholic Kwandong University College of Medicine Simgok-ro 100 Gil 25, Seo-gu, Incheon Metropolitan City, 22711, South Korea.

E-mail addresses: ycna@ish.ac.kr (Y.C. Na), changws0716@yuhs.ac (W.S. Chang).

https://doi.org/10.1016/j.heliyon.2024.e29480
Received 15 September 2023; Received in revised form 1 April 2024; Accepted 8 April 2024
Available online 9 April 2024

1. Introduction

Focused ultrasound (FUS) is a potential non-invasive method that can modulate the blood-brain barrier (BBB) and substantially contribute to drug delivery to the brain [1,2]. The BBB is a specialized and critical structure in the brain that protects the central nervous system (CNS) from harmful substances in the bloodstream [3–5]. Its tight junctions and selective transport mechanisms present a formidable challenge for delivering therapeutic drugs to treat brain diseases effectively. To overcome this obstacle, researchers have explored the use of FUS in combination with microbubbles to transiently and reversibly open the BBB in targeted regions [6–8]. This innovative approach allows for the delivery of drugs and water-soluble macromolecules with a size of several tens of kilodaltons, which were previously restricted by the intact BBB.

The BBB is composed of specific endothelial cells, a basement membrane, pericytes, and astrocytic endfeet [9,10]. The most well-known of these structures is the tight junction, which connects brain endothelial cells [4]. These comprise both tight junction proteins, such as claudin, occludin, and junctional adhesion molecules, as well as scaffolding proteins, such as zonula occludens-1 (ZO-1), which bind to other components to favor strong adhesion [11]. In addition to the paracellular pathway, which is the passage transporting through the BBB owing to these tight junctions, several pathways, including the transcellular pathway, receptor-mediated transcytosis, and cell-mediated transcytosis, can transport molecules through the BBB [12]. Among them, the mechanism of transcellular transport across endothelial cells involves the formation of caveolae, a specific membrane-associated microstructure abundantly expressing caveolin-1 [13,14]. Specifically, the major facilitator superfamily domain-containing 2a (Mfsd2a) protein inhibits transcytosis in CNS endothelial cells [15] and is linked to changes in the lipid composition and caveola formation [16].

The mechanisms of drug delivery facilitated by FUS differ depending on the nature of the drug and the specific transport route. For example, the transcellular lipophilic mechanism allows heroin and theophylline to pass through, whereas D-glucose and L-glutamate are transporter-mediated [17–20]. Furthermore, paracellular leakage through widened tight junctions allows the passage of hydrophilic molecules, whereas transcellular endocytosis allows the passage of large proteins, including DNA/RNA [21,22].

Although FUS holds great promise for enhancing drug delivery through the BBB, its exact mechanism of action remains a subject of ongoing research, and long-term safety evaluations are still limited [23,24]. Several studies that deliver drugs after BBB modulation by FUS have investigated paracellular passage through tight junctions [25,26], and only a few studies have examined transcellular transport across endothelial cells. Therefore, we aimed to investigate whether FUS combined with microbubbles could control other pathways in addition to the paracellular pathway of drug delivery and determine the optimal timing of drug injection according to the

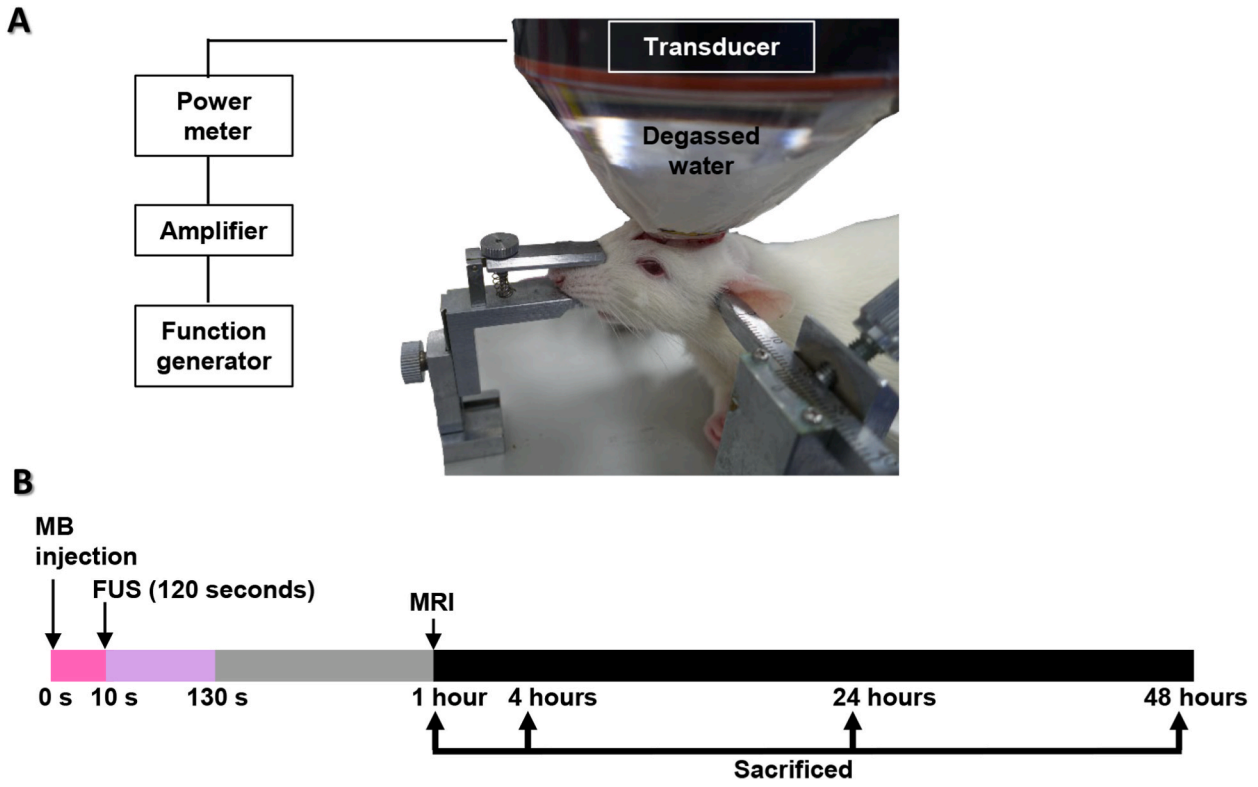

Fig. 1. Experimental FUS system. **(A)** Schematics of the focused ultrasound setup. **(B)** The experiment's timeline for comparison at 1, 4, 24, and 48 h after sonication.
FUS, focused ultrasound; MB, microbubbles; MRI, magnetic resonance imaging.

type of transport.

2. Material and methods

Ethics approval

The Institutional Animal Care and Use Committee of Yonsei University (South Korea) granted approval for all animal studies, which were carried out in compliance with the National Institutes of Health's Guide for the Care and Use of Laboratory Animals (IACUC number: 2019-0208).

2.1. Experimental animals

Animals were kept in cages of groups of three individuals, with a 12/12 h light/dark cycle under regulated humidity and temperature, and received food and water *ad libitum*. One control group (n = 14) and four FUS groups (n = 56, n = 14 per each group) were created from a total of 70 male Sprague–Dawley rats (240–270 g). The rats were euthanized at 1, 4, 24, and 48 h after FUS treatment.

2.2. FUS treatment

A 515-kHz single-element spherically focused H-107MR transducer (focal depth, 51.7 mm; radius of curvature, 63.2 mm; Sonic Concept Inc., Bothell, WA, USA), waveform generator (33220A; Agilent, Palo Alto, CA, USA), and radiofrequency power amplifier (240 L; ENI Inc., Rochester, NY, USA) were used for FUS sonication. Parameters were set as previously described [27]. The transducer assembly was fitted with a cone filled with distilled and degassed water (Fig. 1A). For transducer calibration, a needle-type hydrophone (HNA-0400; Onda, Sunnyvale, CA, USA) was used to measure the acoustic beam profile of the water-filled tank. For a total of 120 s, the average peak-negative pressure was set at 0.2 MPa with a 10-ms burst duration at a 1-Hz pulse-repetition frequency (Fig. 1B).

Before being put in a stereotaxic frame with ear and nose bars, the animals were given a combination of ketamine (75 mg/kg), acepromazine (0.75 mg/kg), and xylazine (4 mg/kg) to induce anesthesia. After the animals' scalps were removed, an ultrasonic transmission gel (ProGel-Dayo Medical Co., Seoul, South Korea) was put to the space between the skull and the cone tip to maximize the ultrasound's efficiency. The FUS target region was the right hippocampal area (anteroposteriorly −3.5; mediolaterally +2.5 from the bregma). Ten seconds before ultrasound sonication, saline-diluted DEFINITY® microbubbles (mean diameter range, 1.1–3.3 μm; Lantheus Medical Imaging, North Billerica, MA, USA) were intravenously administered into the tail vein, and Evans blue (2 %, 100 mg/kg) was intravenously administered at each time point after FUS treatment in the typical rats (n = 7), which were sacrificed 1 h later to examine BBB permeability. In addition, 500-kDa dextran (Thermo Fisher Scientific, Waltham, MA, USA; D7136, R_H = approximately 16 nm) was intravenously administered (1 g/kg) at each time point after sonication (n = 5). The dextran was diluted to 10 mg/mL in

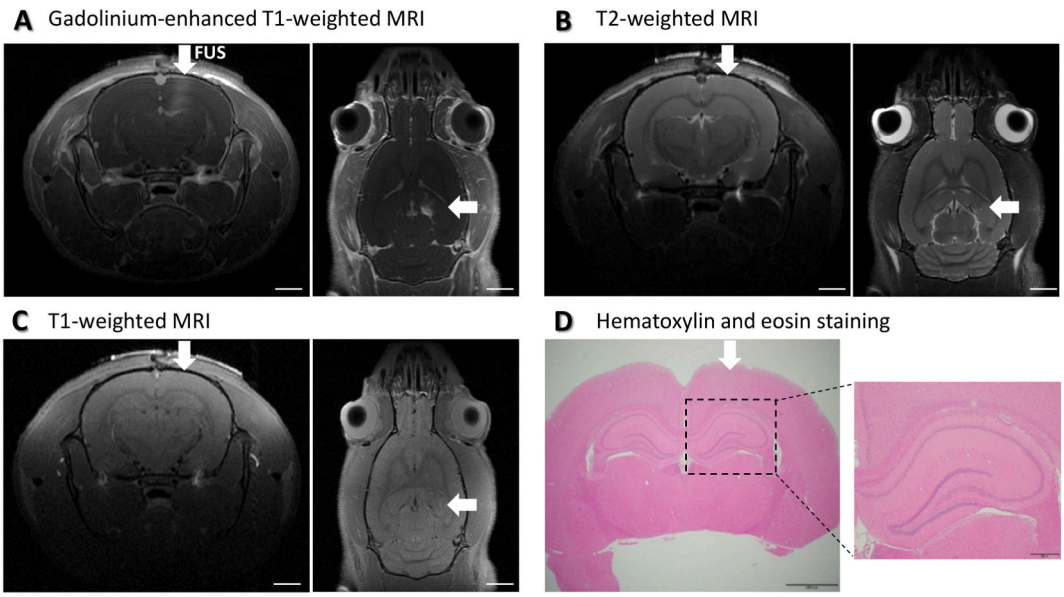

Fig. 2. Confirmation of safe BBB opening by FUS. **(A)** Confirming FUS-mediated opening of the BBB using MRI. Contrast enhancement is visible in gadolinium-enhanced T1-weighted images. BBB opening areas are indicated with an arrow. **(B)** No FUS-mediated edema is observed on T2-weighted MRI scans. **(C)** T1-weighted MRI image. **(D)** Hematoxylin and eosin staining to identify tissue safety. Scale bar: 2000 μm (left) and 500 μm (right). The right side is the enlarged part of the BBB opening.
BBB, blood-brain barrier; FUS, focused ultrasound system; MRI, magnetic resonance imaging.

phosphate-buffered saline.

2.3. Magnetic resonance imaging

An hour after FUS treatment, magnetic resonance imaging (MRI) was performed using a 9.4-T 20-cm bore-diameter MRI system (BioSpec 94/20 USR; Bruker, Ettlingen, Germany) and a rat head coil. A gadolinium-based contrast agent, 0.2 mL/kg Dotarem (gadoterate meglumine; Guerbet, Villepinte, France), was injected into the tail vein. To confirm FUS-mediated BBB permeability, contrast-enhanced T1-weighted images were acquired. However, FUS-induced edema was not observed on T2-weighted images. Moreover, T1-weighted images were obtained without Dotarem contrast (Fig. 2). The MRI sequences used in this study were described in Supplemental Table 1.

2.4. Transmission electron microscopy

The number of caveolae was determined using transmission electron microscopy (TEM). Two samples were extracted from the hippocampus of rats from each group. After securing the hippocampus where the focused ultrasound of the sectioned brain tissue was targeted using an anatomical microscope, the CA1 area of the hippocampus was acquired in a size of 1 mm cubic. Tissues were fixed for 12 h in 2 % glutaraldehyde-paraformaldehyde solution in 0.1 M phosphate buffer (pH 7.4) and then washed in 0.1-M phosphate buffer. Next, tissues were postfixed for 2 h with 1 % OsO_4 dissolved in 0.1-M phosphate buffer, dehydrated using a graded series of ethanol (50–100 %), and infiltrated with propylene oxide. Specimens were embedded using a Poly/Bed 812 kit (Polysciences, Philadelphia, PA, USA) and underwent fresh resin embedding and polymerization for 24 h at 65 °C in an electron microscopy oven (TD-700; Dosaka Em Co., Kyoto, Japan). Tissues were cut into 70-nm-thin sections using Leica EM UC-7 (Leica Microsystems, Wetzlar, Germany) and a diamond knife (Diatome, Hong Kong, China) and were transferred onto copper and nickel grids. All sections were observed using the JEM-1011 transmission electron microscope (JEOL, Tokyo, Japan).

2.5. Histological analysis

Animals were anesthetized and perfused with 0.9 % saline and 4 % paraformaldehyde at 1, 4, 24, and 48 h after FUS sonication. After being extracted and postfixed in 4 % paraformaldehyde (Duksan, Seoul, South Korea) for 3 days at 4 °C, and 30 % sucrose (Duksan) for 3 days at 4 °C. The brains were sectioned into 30 μm using a cryostat (Leica Biosystems, Wetzlar, Germany), and kept at −20 °C in a cryoprotectant solution containing 30 % sucrose, 30 % ethylene glycol (Thermo Fisher Scientific), 1 % polyvinylpyrrolidone (Sigma-Aldrich, St. Louis, MO, USA), and 0.1-M phosphate buffer (pH 7.2).

2.5.1. Immunofluorescence staining

Brain sections were blocked with 5 % normal goat serum (Vector Labs, Burlingame, CA, USA) and incubated with primary antibodies targeting markers for caveolae (caveolin-1; ab2910; 1:200; Abcam, Cambridge, UK) and endothelial cells (Reca1; MCA970R; 1:150; Serotec, Oxford, UK) at 4 °C overnight in order to detect caveolin-1 and endothelial cells. The sections were incubated for 2 h at 25 °C with the following secondary antibodies: Alexa Fluor 488 (A11008; 1:300; Thermo Fisher Scientific) and Alexa Fluor 594 (A11005; 1:300; Thermo Fisher Scientific). The 4′,6-diamidino-2-phenylindole mounting media (Vector Laboratories) was used to mount each section. A Zeiss Axio Imager M2 microscope (Carl Zeiss, Oberkochen, Germany) was used for taking fluorescent images.

2.5.2. Hematoxylin and eosin staining

Hematoxylin and eosin (H&E) staining was used to evaluate hemorrhage and injury. Prior to H&E staining, brains were fixed in paraffin wax and sliced into 4 μm sections. An optical microscope was used to observe the tissues (BX51; Olympus, Tokyo, Japan).

2.6. Western blot analysis

After the rats' brains were removed, the hippocampus was cut out using a 1-mm coronal brain slicer matrix. To extract the proteins, the tissues were homogenized with lysis buffer (PRO-PREP; iNtRON Biotechnology, Seongnam, Korea) and centrifuged for at 12 000 rpm for 20 min. Protein concentration in the supernatant was measured using a Pierce bicinchoninic acid Protein Assay Kit (Thermo Fisher Scientific). Proteins were separated using 12 % sodium dodecyl sulfate-polyacrylamide gels and transferred onto polyvinylidene fluoride membranes. After blocking using a solution containing 5 % non-fat dry milk, the membranes were incubated overnight at 4 °C with primary antibodies against ZO-1 (61–7300; 1:1000; Thermo Fisher Scientific), occludin (ab167161; 1:5000; Abcam), Mfsd2a (ab177881; 1:1000; Abcam), caveolin-1 (ab2910; 1:1000; Abcam), and β-actin (1:20 000; Sigma-Aldrich). The membranes were then incubated for 2 h at 25 °C with secondary antibodies with goat anti-rabbit immunoglobulin (Ig)G(H + L)-HRP (1:2000 for ZO-1, Mfsd2a, and caveolin-1; 1:10 000 for occludin; GenDEPOT, Katy, TX, USA) and goat anti-mouse IgG(H + L)-HRP (1:20 000 for β-actin; GenDEPOT). The proteins were obtained through a chemiluminescence solution (WEST-Queen; iNtRON Biotechnology) and the ImageQuant LAS 4000 (GE Healthcare Life Sciences, Chicago, IL, USA). The signals were evaluated using an analytical system (Multi Gauge version 3.0; Fujifilm, Tokyo, Japan).

2.7. Statistical analysis

Tukey's post-hoc comparisons were used in conjunction with one-way analysis of variance to examine the data, and GraphPad Prism 7 (GraphPad Software, Inc., San Diego, CA, USA) was used for statistical analysis. The mean ± standard error of the mean is used to show the data. Statistical significance was set at $^{*}P < 0.05$, $^{**}P < 0.01$, and $^{***}P < 0.001$.

3. Results

3.1. Increased BBB permeability after FUS

One hour after sonication, MRI was performed to confirm the signal change in the targeted right hippocampus. Contrast-enhanced T1-weighted images confirmed that the BBB of the targeted region was opened (Fig. 2A). T2-weighted and T1-weighted images showed that FUS did not cause edema (Fig. 2B and C). H&E staining showed no red blood cell outflow, which demonstrates absence of cerebral hemorrhage caused by microbubbles (Fig. 2D). In addition, Evans blue was locally leaked only to the FUS-targeted site, thereby confirming the permeability of the BBB along with its closure in 24 h. Evans blue is 961 Da, a size that cannot penetrate the BBB, confirmed by the inability of Evans blue dye penetration in the control group that was not treated with FUS (Fig. 3A). In addition, we confirmed that 500-kDa dextran molecules, which are larger than Evans blue molecules, leaked for up to 1, 4, and even 24 h after FUS treatment (Fig. 3D).

3.2. Increased paracellular pathway through loosening of tight junctions

Our results indicate that the levels of ZO-1 and occludin were the lowest at 1 h after sonication, with gradual recovery to the pre-

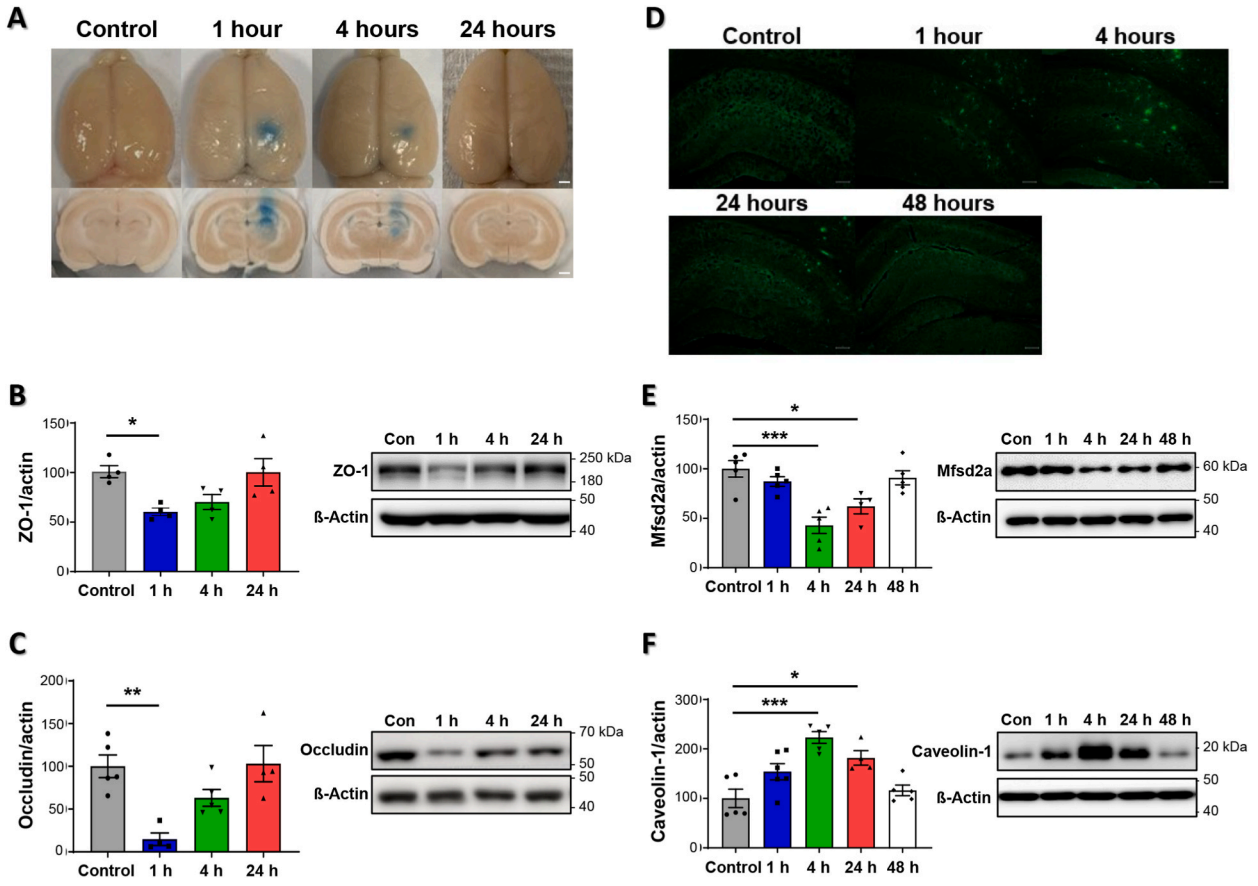

Fig. 3. Comparison of time points by molecular size during BBB opening between the control and focused ultrasound system groups. **(A)** Extravasation of Evans blue in the brain. **(B, C)** Changes of ZO-1 and occludin using Western blot. **(D)** Quantity comparison of 500-kDa dextran transport. Scale bar: 200 μm. **(E, F)** Comparison of Mfsd2a and caveolin-1 levels using Western blot. Data are expressed as the mean ± standard error of the mean (n = 4–6 per group). $^{*}P < 0.05$, $^{**}P < 0.01$, $^{***}P < 0.001$; data are analyzed by one-way ANOVA with Tukey's post-hoc comparisons. ANOVA, analysis of variance; BBB, blood-brain barrier; Mfsd2a, major facilitator superfamily domain-containing 2a; ZO-1, zonula occludens-1. (For interpretation of the references to colour in this figure legend, the reader is referred to the Web version of this article.)

sonication levels. Based on Western blot analysis, the levels of ZO-1 were significantly lower than those of the control group after 1 h of FUS treatment ($P = 0.028$), and levels of occludin were significantly lower than those of the control group after 1 h of FUS treatment ($P = 0.0027$) (Fig. 3).

The expression of Evans blue that was able to penetrate the right hippocampal area was at its highest at 1 h after FUS treatment but returned to control levels at 24 h after FUS treatment (Fig. 3). The presence of tight junctions was confirmed by TEM imaging in the control and all FUS-targeted tissues, with tight junctions being the most relaxed in the 1-h post-FUS group (Supplementary Fig. 1).

3.3. Enhanced transcellular pathway through Caveola formation

Caveolae levels started to increase 1 h after FUS (Fig. 4C and D) and reached their peak at 4 h after FUS (Fig. 4E and F). At this stage, caveolae were observed to be in the process of transcytosis, indicating that the most active state of the transcellular pathway occurred 4 h after sonication. Compared to the control state (Fig. 4A and B), the caveolae maintained their formation for up to 24 h (Fig. 4G and H) and finally returned to a normal state at 48 h after sonication (Fig. 4I and J).

Four hours after FUS treatment, caveolin-1 levels peaked, whereas Mfsd2a levels reached their lowest values. Based on Western blot analysis, Mfsd2a levels at 4 h and 24 h after FUS treatment were significantly lower than that of the control ($P = 0.0002$ and $P = 0.0175$, respectively); those of caveolin-1 at 4 h and 24 h after FUS treatment were significantly higher than that of the control ($P = 0.0001$ and $P = 0.013$, respectively) (Fig. 3). Four hours after FUS treatment, the amount of 500-kDa dextran passing through the right hippocampal region peaked, and 48 h after FUS treatment, it recovered to control levels (Fig. 3). Thus, levels of tight junction proteins decreased immediately at 1 h after FUS treatment (Fig. 3), while the number of caveolae peaked at 4 h after FUS treatment (Fig. 4), indicating the time interval between tight junction loosening and caveola-mediated transcytosis.

The levels of both caveolin-1, a marker of caveolae, and Reca1, a marker of endothelial cells, were shown to be increased in FUS-treated rats compared to untreated rats, according to immunohistochemical analysis. Caveolin-1 and Reca1 were co-localized primarily in the same endothelial area (Fig. 5), indicating that caveolin-1 is expressed in endothelial cells.

4. Discussion

Currently, research on minimally invasive and reversible opening of the BBB through FUS is actively being conducted [17,20].

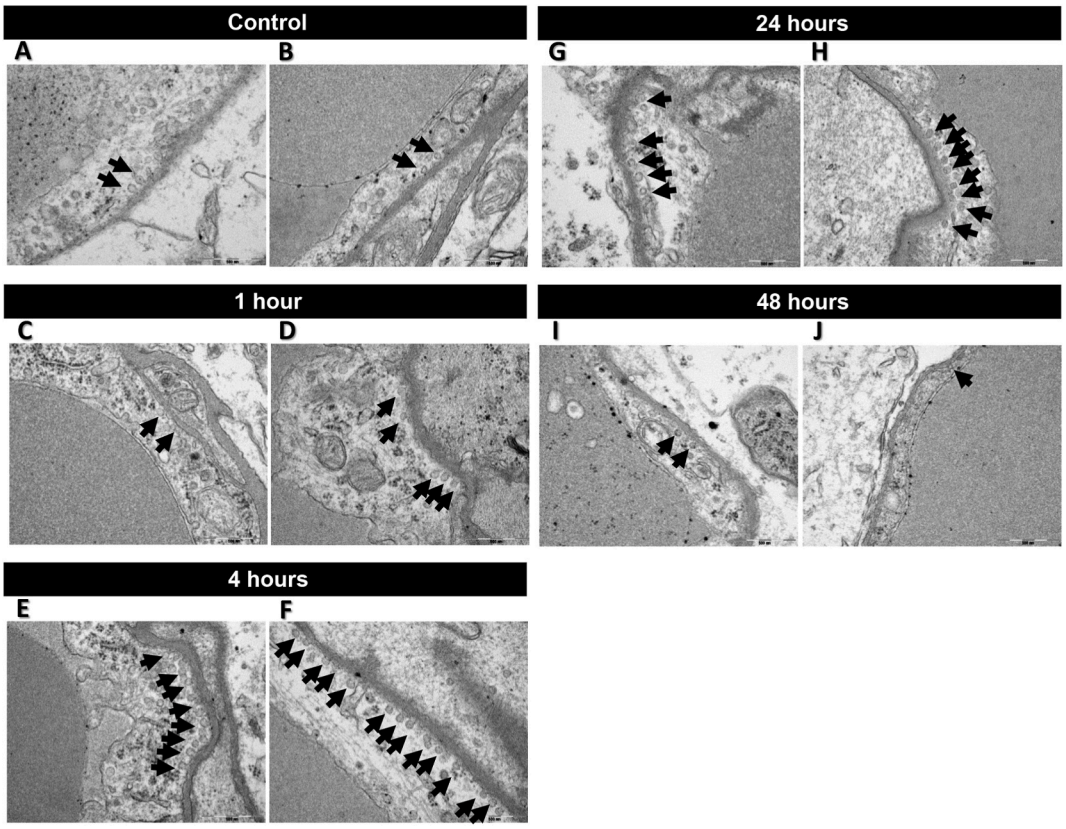

Fig. 4. Electron microscopic examination of caveola formation (arrowheads). **(A, B)** Control group, **(C, D)** 1 h, **(E, F)** 4 h, **(G, H)** 24 h, and **(I, J)** 48 h after sonication. Scale bar: 500 nm.

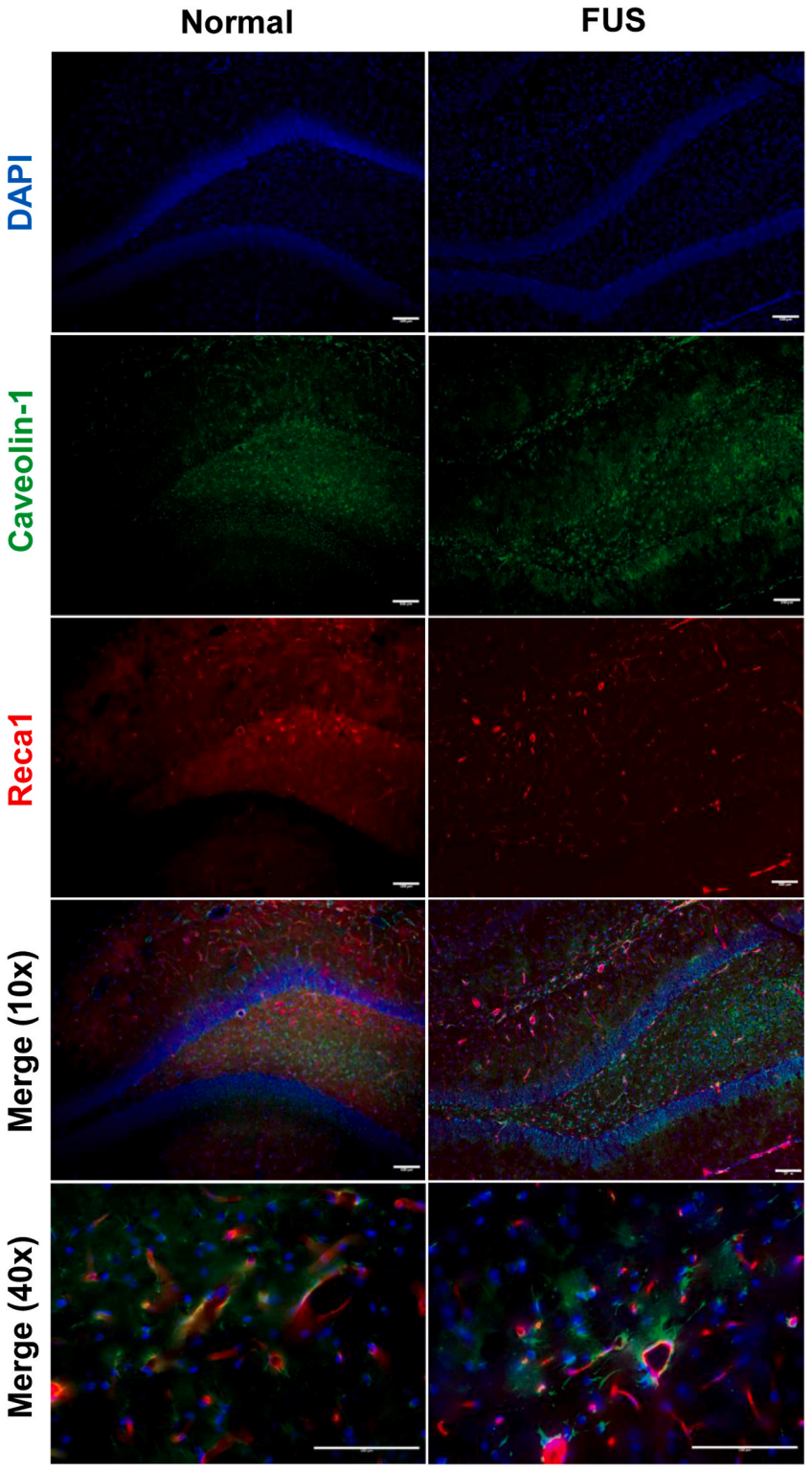

Fig. 5. Immunohistochemical examination of caveolin-1 and Reca1. Co-localization of caveolin-1 and Reca1: FUS-treated rats show higher amounts of both caveolin-1 and Reca1 than with untreated rats. Scale bar: 100 μm.
DAPI, 4′,6-diamidino-2-phenylindole; FUS, focused ultrasound.

However, the exact mechanism of action of this method remains unclear [7,27]. Therefore, an increased understanding of the cellular and molecular pathways involved in FUS-mediated BBB opening is required to improve drug delivery to the CNS.

4.1. Enhanced paracellular delivery via BBB modulation

Early studies on the mechanisms of BBB opening using FUS have focused on the paracellular pathway [28,29]. This transport process is suggested to be induced by microbubbles, which cause shear stress in endothelial cells [30], thus temporarily opening the BBB. In the existing studies exploring the BBB opening through FUS, a predominant focus has been on the loosening of tight junctions as the main mechanism facilitating drug delivery [25,26]. The disruption of tight junctions allows for increased paracellular leakage, thereby enabling the delivery of water-soluble large molecules that were previously restricted by the intact BBB.

Several studies have demonstrated the successful delivery of large molecules across the BBB following FUS treatment in preclinical models. For instance, one study demonstrated the delivery of large protein-based therapeutics, including antibodies and enzymes, into the brain parenchyma by exploiting the FUS-mediated BBB opening [25]. Other studies have identified the possibility of FUS for dopamine D (4) receptor target antibodies to pass through the BBB after FUS to treat neurodegenerative diseases, and antibodies to amyloid-β have increased transmission to the brain, weakening cognitive deficits in Alzheimer's disease [31,32].

To check for tight junction loosening, some studies confirmed that the levels of occludin and ZO-1 were significantly decreased 1 h after sonication [26], which is consistent with our results. Although the loosening of tight junctions has shown significant potential in enhancing the delivery of large molecules, it is essential to acknowledge that FUS-assisted BBB opening is a complex process involving multiple mechanisms beyond paracellular leakage.

4.2. Enhanced transcytosis via BBB modulation

We also explored whether FUS can modulate other mechanisms of BBB opening such as vesicle-mediated transport, particularly through caveolae, which are small membrane invaginations rich in lipid-anchoring proteins, glycosphingolipids, and cholesterol [33]. Specifically, caveolae are related to the transcellular movement of macromolecules, such as albumin and lipoproteins [34]. As the main vesicle transporter of endothelial cells, caveola constituted of caveolin-1 are membrane invaginations measuring 50–100 nm in

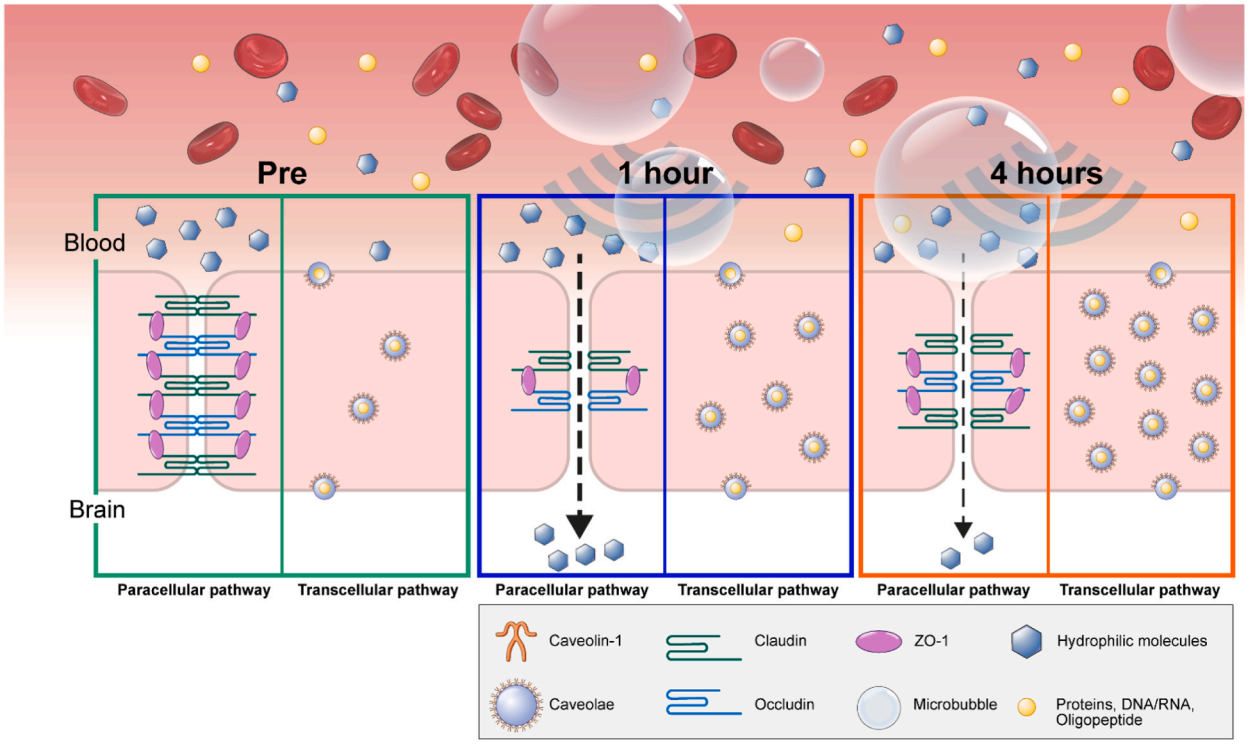

Fig. 6. Time gap in peak activity between the paracellular and transcellular pathways.
The BBB interferes with drug delivery as a homeostatic barrier, whereas FUS may modulate BBB permeability to enable drug delivery. After FUS sonication, the paracellular pathway is activated at 1 h, and the transcytosis pathway reaches peak activity at 4 h after FUS treatment. Tight junction proteins are downregulated following FUS usually at 1 h; thus, hydrophilic molecules could pass through the BBB. Caveolae are associated with transcytosis and can deliver plasma proteins with the most active transcytosis 4 h after FUS treatment.BBB, blood-brain barrier; FUS, focused ultrasound; Pre, pre-sonication; ZO-1, zonula occludens-1.

diameter that selectively endocytose macromolecules across cells (e.g., size >3 nm) [35,36]. It is thought that alterations in lipid content and caveola development in endothelial cells are related to the Mfsd2a transmembrane protein, which is expressed exclusively in vascular endothelial cells [15,16]. Mfsd2a transports docosahexaenoic acid into endothelial cells, which blocks caveolae from forming in the BBB [37]. Research on *Mfsd2a*-knockout mice showed that the absence of Mfsd2a increases BBB permeability and brain endothelial cell vesicular transcytosis without affecting tight junctions [37]. Therefore, understanding the role of Mfsd2a can contribute to the development of effective drug delivery methods for treating CNS disorders, including neurodegenerative diseases [38]. A few reports have indicated that caveolin-1 expression increases following ultrasound treatment in both animals and *in vitro* models [18,19]. Furthermore, a study suggested a similar finding and showed that caveolin-1 has a crucial role in the transportation of large (500 kDa), but not smaller (3 and 70 kDa) cargoes [39].

Our study observed an increase in the number of caveolae after FUS through TEM (Fig. 4). Additionally, we observed an increase in cavolin-1 and a decrease in Mfsd2a levels through Western blot experiments for quantification, and as a result, we suggested that 4 h after FUS treatment was the peak time (Fig. 3). This indicates that the decrease in the level of regulatory Mfsd2a is associated with an increase in the level of caveolin-1, which subsequently increases the number of caveolae available for caveolin-mediated transcytosis through the transcellular pathway. Dextran, a large molecule with a 500-kDa size, was also demonstrated to have passed through the BBB.

4.3. Time gap between paracellular and transcellular delivery

In addition to the aforementioned results, we conducted research on whether the timing for achieving maximum effectiveness would be the same if FUS regulates the BBB through two different mechanisms. According to our results, tight junction protein levels were at their lowest 1 h after FUS treatment, began to recover at 4 h after FUS treatment, and reached their control levels at the 24-h after FUS time point. Specifically, caveolin-1 and Mfsd2a levels peaked at 4 h after FUS treatment and returned to normal levels at 48 h after FUS treatment, indicating activation of transcytosis-mediated transport. Indeed, Evans blue passing through the BBB via the paracellular mechanism showed the most penetration at 1 h after FUS treatment, as shown in the TJP results, although 500-kDa dextran molecules passing through the BBB via the transcytosis mechanism had the best delivery efficiency at 4 h after FUS treatment (Fig. 3). This suggest that there is a time gap in delivery through the paracellular and transcellular pathways (Fig. 6).

These findings align with those of a previous study that suggested different temporal dynamics of leakage might be at play in FUS-induced BBB opening. Particularly, fast leakage would reach extracellular peak intensity during sonication, whereas slow leakage would only begin 5–15 min after FUS treatment and occur along the vessel length [40]. According to the authors' conjectures, fast and slow leakage could be carried out through paracellular and transcellular transports, respectively [41].

In another previous study, Deng et al. reported that modulation of the transcellular pathway by FUS studied to date only observed an increase in caveolin-1 and caveolae formation, which was confirmed 1 h after sonication [18]. Compared with the report by Deng et al., our study confirmed various time-based observations of FUS-induced effects and whether FUS affects Mfsd2a, which is considered one of the cellular signaling pathways, rather than mechanistically generated in caveolae formation. Moreover, the decrease in tight junction protein levels supports the hypothesis that molecules paracellularly move through the opened BBB after FUS. The extravasation of Evans blue into the brain parenchyma, which is used as a method of confirming BBB permeability by ultrasound [27,42], was also confirmed with the same result.

Importantly, the time gap between these two pathways offers valuable insights into efficient drug delivery. Molecules transported via transcytosis would be more effective 4 h after BBB opening, whereas those transported via the paracellular route would be more effective 1 h after sonication. Consequently, the optimal delivery time for bigger or lipophilic compounds may be 4 h after sonication, whereas that for smaller or hydrophilic molecules may be 1 h after FUS treatment.

This has practical implications for clinical drug delivery, as different drugs require specific timing for optimal delivery based on their characteristics. In clinical practice, drugs such as mannitol, transported through the paracellular pathway, are best delivered immediately after BBB opening, whereas drugs such as Moriah 1000, made from proteins, DNA/RNA, and oligopeptides, are transported through adsorptive-mediated transcytosis [41,43,44]. It is best delivered 4 h after FUS treatment. This knowledge could be useful for establishing optimal treatment guidelines. Therefore, the timing of drug injection should be carefully selected according to the components of the compound to be delivered.

This study has a few limitations that require acknowledgment. First, whether the time points of 1, 4, 24, and 48 h that we set were the most optimal is unknown. In fact, some studies have reported that delivery through the paracellular mechanism is better immediately, although specifying the optimal timing according to each mechanism was difficult in this study [45]. However, since a time gap was observed, further research is needed. Second, other methods exist, such as the receptor-mediated method, in addition to the two methods that we studied for delivery through the BBB [46]. Studying the FUS effect of this mechanism seems necessary. Third, a difference in drug delivery efficiency according to BBB control was observed, although how much these differences affect disease treatment is unknown. However, in this study, only the hippocampus area was targeted and evaluated, so there is a limitation when trying to deliver drugs to other areas of the brain. Therefore, research is needed to verify differences in treatment effects according to drug penetration efficiency by applying these characteristics in specific animal models.

5. Conclusions

Our study provides evidence for multiple pathways across the BBB that can be stimulated by FUS, including paracellular transport and caveola-mediated transcytosis. We identified a time gap between the initiation of paracellular and transcellular transports after

FUS. Loosening of tight junction proteins was at the lowest 1 h after FUS treatment and recovered at 24 h after FUS treatment, whereas the caveola formation involved in the transcellular pathway reached a peak at 4 h after FUS treatment and recovered at 48 h after FUS treatment. In the future, FUS could have applications in various fields such as stem cell treatment and genetics [47]. When delivering a drug after BBB opening induced by FUS, injection times should be carefully determined depending on the drug's characteristics to establish optimal treatment guidelines.

Funding

This work was supported by the National Research Foundation of Korea (NRF) funded by the Ministry of Education [grant numbers 2016R1D1A3B03932649 and 2019R1I1A3A01043477]; the Ministry of Science and ICT [grant number RS-2023-00266075]; and the Korea Medical Device Development Fund [grant number RS-2020-KD000103].

Data Availability statement

Not applicable.

CRediT authorship contribution statement

Younghee Seo: Writing – original draft, Methodology. **Kyung Won Chang:** Writing – original draft. **Jihyeon Lee:** Methodology. **Chanho Kong:** Investigation. **Jaewoo Shin:** Investigation. **Jin Woo Chang:** Supervision. **Young Cheol Na:** Writing – review & editing, Funding acquisition, Conceptualization. **Won Seok Chang:** Writing – review & editing, Funding acquisition, Conceptualization.

Declaration of competing interest

The authors declare that they have no known competing financial interests or personal relationships that could have appeared to influence the work reported in this paper.

Acknowledgments

We would like to thank Dong-Su Jang, MFA (medical illustrator, Medical Research Support Section, Yonsei University College of Medicine) for his assistance with our illustrations.

Appendix A. Supplementary data

Supplementary data to this article can be found online at https://doi.org/10.1016/j.heliyon.2024.e29480.

References

[1] L. Bakay, H.T. Ballantine, T.F. Hueter, D. Sosa, Ultrasonically produced changes in the blood-brain barrier, AMA Arch Neurol Psychiatry 76 (1956) 457–467, https://doi.org/10.1001/archneurpsyc.1956.02330290001001.
[2] K. Hynynen, N. McDannold, N. Vykhodtseva, F.A. Jolesz, Noninvasive MR imaging-guided focal opening of the blood-brain barrier in rabbits, Radiology 220 (2001) 640–646, https://doi.org/10.1148/radiol.2202001804.
[3] R. Pandit, L. Chen, J. Götz, The blood-brain barrier: physiology and strategies for drug delivery, Adv. Drug Deliv. Rev. 165–166 (2020) 1–14, https://doi.org/10.1016/j.addr.2019.11.009.
[4] W.M. Pardridge, The blood-brain barrier: bottleneck in brain drug development, NeuroRx 2 (2005) 3–14, https://doi.org/10.1602/neurorx.2.1.3.
[5] W.M. Pardridge, CSF, blood-brain barrier, and brain drug delivery, Expert Opin Drug Deliv 13 (2016) 963–975, https://doi.org/10.1517/17425247.2016.1171315.
[6] J. Lee, W.S. Chang, J. Shin, Y. Seo, C. Kong, B.W. Song, Y.C. Na, B.S. Kim, J.W. Chang, Non-invasively enhanced intracranial transplantation of mesenchymal stem cells using focused ultrasound mediated by overexpression of cell-adhesion molecules, Stem Cell Res. 43 (2020) 101726, https://doi.org/10.1016/j.scr.2020.101726.
[7] N. McDannold, C.D. Arvanitis, N. Vykhodtseva, M.S. Livingstone, Temporary disruption of the blood-brain barrier by use of ultrasound and microbubbles: safety and efficacy evaluation in rhesus macaques, Cancer Res. 72 (2012) 3652–3663, https://doi.org/10.1158/0008-5472.CAN-12-0128.
[8] J. Shin, C. Kong, J. Lee, B.Y. Choi, J. Sim, C.S. Koh, M. Park, Y.C. Na, S.W. Suh, W.S. Chang, J.W. Chang, Focused ultrasound-induced blood-brain barrier opening improves adult hippocampal neurogenesis and cognitive function in a cholinergic degeneration dementia rat model, Alzheimer's Res. Ther. 11 (2019) 110, https://doi.org/10.1186/s13195-019-0569-x.
[9] N.J. Abbott, L. Rönnbäck, E. Hansson, Astrocyte-endothelial interactions at the blood-brain barrier, Nat. Rev. Neurosci. 7 (2006) 41–53, https://doi.org/10.1038/nrn1824.
[10] R. Daneman, A. Prat, The blood-brain barrier, Cold Spring Harb Perspect Biol 7 (2015) a020412, https://doi.org/10.1101/cshperspect.a020412.
[11] M. Saitou, M. Furuse, H. Sasaki, J.D. Schulzke, M. Fromm, H. Takano, T. Noda, S. Tsukita, Complex phenotype of mice lacking occludin, a component of tight junction strands, Mol. Biol. Cell 11 (2000) 4131–4142, https://doi.org/10.1091/mbc.11.12.4131.
[12] N. Hartl, F. Adams, O.M. Merkel, From adsorption to covalent bonding: apolipoprotein E functionalization of polymeric nanoparticles for drug delivery across the blood-brain barrier, Adv. Ther. 4 (2021) 2000092, https://doi.org/10.1002/adtp.202000092.

[13] B.L. Coomber, P.A. Stewart, Morphometric analysis of CNS microvascular endothelium, Microvasc. Res. 30 (1985) 99–115, https://doi.org/10.1016/0026-2862(85)90042-1.
[14] D. Virgintino, D. Robertson, M. Errede, V. Benagiano, U. Tauer, L. Roncali, M. Bertossi, Expression of caveolin-1 in human brain microvessels, Neuroscience 115 (2002) 145–152, https://doi.org/10.1016/s0306-4522(02)00374-3.
[15] A. Ben-Zvi, B. Lacoste, E. Kur, B.J. Andreone, Y. Mayshar, H. Yan, C. Gu, Mfsd2a is critical for the formation and function of the blood-brain barrier, Nature 509 (2014) 507–511, https://doi.org/10.1038/nature13324.
[16] B.J. Andreone, B.W. Chow, A. Tata, B. Lacoste, A. Ben-Zvi, K. Bullock, A.A. Deik, D.D. Ginty, C.B. Clish, C. Gu, Blood-brain barrier permeability is regulated by lipid transport-dependent suppression of caveolae-mediated transcytosis, Neuron 94 (2017) 581–594.e5, https://doi.org/10.1016/j.neuron.2017.03.043.
[17] N. Sheikov, N. McDannold, N. Vykhodtseva, F. Jolesz, K. Hynynen, Cellular mechanisms of the blood-brain barrier opening induced by ultrasound in presence of microbubbles, Ultrasound Med. Biol. 30 (2004) 979–989, https://doi.org/10.1016/j.ultrasmedbio.2004.04.010.
[18] J. Deng, Q. Huang, F. Wang, Y. Liu, Z. Wang, Z. Wang, Q. Zhang, B. Lei, Y. Cheng, The role of caveolin-1 in blood-brain barrier disruption induced by focused ultrasound combined with microbubbles, J. Mol. Neurosci. 46 (2012) 677–687, https://doi.org/10.1007/s12031-011-9629-9.
[19] V. Lionetti, A. Fittipaldi, S. Agostini, M. Giacca, F.A. Recchia, E. Picano, Enhanced caveolae-mediated endocytosis by diagnostic ultrasound in vitro, Ultrasound Med. Biol. 35 (2009) 136–143, https://doi.org/10.1016/j.ultrasmedbio.2008.07.011.
[20] D.S. Hersh, B.A. Nguyen, J.G. Dancy, A.R. Adapa, J.A. Winkles, G.F. Woodworth, A.J. Kim, V. Frenkel, Pulsed ultrasound expands the extracellular and perivascular spaces of the brain, Brain Res. 1646 (2016) 543–550, https://doi.org/10.1016/j.brainres.2016.06.040.
[21] W.M. Pardridge, A historical review of brain drug delivery, Pharmaceutics 14 (2022) 1283, https://doi.org/10.3390/pharmaceutics14061283.
[22] R.I. Teleanu, M.D. Preda, A.G. Niculescu, O. Vladăcenco, C.I. Radu, A.M. Grumezescu, D.M. Teleanu, Current strategies to enhance delivery of drugs across the blood-brain barrier, Pharmaceutics 14 (2022) 987, https://doi.org/10.3390/pharmaceutics14050987.
[23] D.G. Blackmore, F. Turpin, A.Z. Mohamed, F. Zong, R. Pandit, M. Pelekanos, F. Nasrallah, P. Sah, P.F. Bartlett, J. Götz, Multimodal analysis of aged wild-type mice exposed to repeated scanning ultrasound treatments demonstrates long-term safety, Theranostics 8 (2018) 6233–6247, https://doi.org/10.7150/thno.27941.
[24] M.E. Downs, A. Buch, M.E. Karakatsani, E.E. Konofagou, V.P. Ferrera, Blood-brain barrier opening in behaving non-human primates via focused ultrasound with systemically administered microbubbles, Sci. Rep. 5 (2015) 15076, https://doi.org/10.1038/srep15076.
[25] A. Burgess, K. Shah, O. Hough, K. Hynynen, Focused ultrasound-mediated drug delivery through the blood-brain barrier, Expert Rev. Neurother. 15 (2015) 477–491, https://doi.org/10.1586/14737175.2015.1028369.
[26] N. Sheikov, N. McDannold, S. Sharma, K. Hynynen, Effect of focused ultrasound applied with an ultrasound contrast agent on the tight junctional integrity of the brain microvascular endothelium, Ultrasound Med. Biol. 34 (2008) 1093–1104, https://doi.org/10.1016/j.ultrasmedbio.2007.12.015.
[27] J. Shin, C. Kong, J.S. Cho, J. Lee, C.S. Koh, M.S. Yoon, Y.C. Na, W.S. Chang, J.W. Chang, Focused ultrasound-mediated noninvasive blood-brain barrier modulation: preclinical examination of efficacy and safety in various sonication parameters, Neurosurg. Focus 44 (2018) E15, https://doi.org/10.3171/2017.11.FOCUS17627.
[28] W.Y. Chai, P.C. Chu, M.Y. Tsai, Y.C. Lin, J.J. Wang, K.C. Wei, Y.Y. Wai, H.L. Liu, Magnetic-resonance imaging for kinetic analysis of permeability changes during focused ultrasound-induced blood-brain barrier opening and brain drug delivery, J Control Release 192 (2014) 1–9, https://doi.org/10.1016/j.jconrel.2014.06.023.
[29] M.A. O'Reilly, O. Hough, K. Hynynen, Blood-brain barrier closure time after controlled ultrasound-induced opening is independent of opening volume, J. Ultrasound Med. 36 (2017) 475–483, https://doi.org/10.7863/ultra.16.02005.
[30] H. Chen, W. Kreider, A.A. Brayman, M.R. Bailey, T.J. Matula, Blood vessel deformations on microsecond time scales by ultrasonic cavitation, Phys. Rev. Lett. 106 (2011) 034301, https://doi.org/10.1103/PhysRevLett.106.034301.
[31] C. Greene, M. Campbell, Tight junction modulation of the blood brain barrier: CNS delivery of small molecules, Tissue Barriers 4 (2016) e1138017, https://doi.org/10.1080/21688370.2015.1138017.
[32] M. Kinoshita, N. McDannold, F.A. Jolesz, K. Hynynen, Targeted delivery of antibodies through the blood-brain barrier by MRI-guided focused ultrasound, Biochem. Biophys. Res. Commun. 340 (2006) 1085–1090, https://doi.org/10.1016/j.bbrc.2005.12.112.
[33] M. De Bock, V. Van Haver, R.E. Vandenbroucke, E. Decrock, N. Wang, L. Leybaert, Into rather unexplored terrain-transcellular transport across the blood-brain barrier, Glia 64 (2016) 1097–1123, https://doi.org/10.1002/glia.22960.
[34] V.M. Pulgar, Transcytosis to cross the blood brain barrier: new advancements and challenges, Front. Neurosci. 12 (2018) 1019, https://doi.org/10.3389/fnins.2018.01019.
[35] Y. Komarova, A.B. Malik, Regulation of endothelial permeability via paracellular and transcellular transport pathways, Annu. Rev. Physiol. 72 (2010) 463–493, https://doi.org/10.1146/annurev-physiol-021909-135833.
[36] Z. Wang, C. Tiruppathi, J. Cho, R.D. Minshall, A.B. Malik, Delivery of nanoparticle: complexed drugs across the vascular endothelial barrier via caveolae, IUBMB Life 63 (2011) 659–667, https://doi.org/10.1002/iub.485.
[37] Y.R. Yang, X.Y. Xiong, J. Liu, L.R. Wu, Q. Zhong, K. Zhou, Z.Y. Meng, L. Liu, F.X. Wang, Q.W. Gong, M.F. Liao, C.M. Duan, J. Li, M.H. Yang, Q. Zhang, C.X. Gong, Q.W. Yang, Mfsd2a (Major Facilitator Superfamily Domain Containing 2a) attenuates intracerebral hemorrhage-induced blood-brain barrier disruption by inhibiting vesicular transcytosis, J. Am. Heart Assoc. 6 (2017) e005811, https://doi.org/10.1161/JAHA.117.005811.
[38] M.D. Sweeney, Z. Zhao, A. Montagne, A.R. Nelson, B.V. Zlokovic, Blood-brain barrier: from physiology to disease and back, Physiol. Rev. 99 (2019) 21–78, https://doi.org/10.1152/physrev.00050.2017.
[39] R. Pandit, W.K. Koh, R.K.P. Sullivan, T. Palliyaguru, R.G. Parton, J. Götz, Role for caveolin-mediated transcytosis in facilitating transport of large cargoes into the brain via ultrasound, J Control Release 327 (2020) 667–675, https://doi.org/10.1016/j.jconrel.2020.09.015.
[40] B. Oller-Salvia, M. Sánchez-Navarro, E. Giralt, M. Teixidó, Blood-brain barrier shuttle peptides: an emerging paradigm for brain delivery, Chem. Soc. Rev. 45 (2016) 4690–4707, https://doi.org/10.1039/c6cs00076b.
[41] E.E. Cho, J. Drazic, M. Ganguly, B. Stefanovic, K. Hynynen, Two-photon fluorescence microscopy study of cerebrovascular dynamics in ultrasound-induced blood-brain barrier opening, J Cereb Blood Flow Metab 31 (2011) 1852–1862, https://doi.org/10.1038/jcbfm.2011.59.43.D.G.
[42] F. Turpin Blackmore, T. Palliyaguru, H.T. Evans, A. Chicoteau, W. Lee, M. Pelekanos, N. Nguyen, J. Song, R.K.P. Sullivan, P. Sah, P.F. Bartlett, J. Götz, Low-intensity ultrasound restores long-term potentiation and memory in senescent mice through pleiotropic mechanisms including NMDAR signaling, Mol Psychiatry 26 (2021) 6975–6991, https://doi.org/10.1038/s41380-021-01129-7.
[43] S.I. Rapoport, Osmotic opening of the blood-brain barrier: principles, mechanism, and therapeutic applications, Cell. Mol. Neurobiol. 20 (2000) 217–230, https://doi.org/10.1023/a:1007049806660.
[44] G.C. Terstappen, A.H. Meyer, R.D. Bell, W. Zhang, Strategies for delivering therapeutics across the blood-brain barrier, Nat. Rev. Drug Discov. 20 (2021) 362–383, https://doi.org/10.1038/s41573-021-00139-y.
[45] D. Günzel, A.S. Yu, Claudins and the modulation of tight junction permeability, Physiol. Rev. 93 (2013) 525–569, https://doi.org/10.1152/physrev.00019.2012.
[46] J. Wang, Z. Li, M. Pan, M. Fiaz, Y. Hao, Y. Yan, L. Sun, F. Yan, Ultrasound-mediated blood-brain barrier opening: an effective drug delivery system for theranostics of brain diseases, Adv. Drug Deliv. Rev. 190 (2022) 114539, https://doi.org/10.1016/j.addr.2022.114539.
[47] D. McMahon, R. Bendayan, K. Hynynen, Acute effects of focused ultrasound-induced increases in blood-brain barrier permeability on rat microvascular transcriptome, Sci. Rep. 7 (2017) 45657, https://doi.org/10.1038/srep45657.